Journal of Power Sources 196 (2011) 7533–7540

Contents lists available at ScienceDirect

Journal of Power Sources

journal homepage: www.elsevier.com/locate/jpowsour

A self-pumping and self-breathing micro direct methanol fuel cell with polymer bipolar plates

Lingjun Sun[a,b], Chong Liu[a,*], Junsheng Liang[a], Xuelin Zhu[b], Tianhong Cui[b,**]

[a] Key Laboratory for Micro/Nano Technology and System of Liaoning Province, Dalian University of Technology, Dalian, Liaoning 116023, China
[b] Department of Mechanical Engineering, University of Minnesota, Minneapolis, MN 55455, USA

ARTICLE INFO

Article history:
Received 17 December 2010
Received in revised form 15 March 2011
Accepted 18 March 2011
Available online 12 April 2011

Keywords:
Direct methanol fuel cell
Self-pumping
Polymer
Hot embossing

ABSTRACT

A passive micro direct methanol fuel cell (DMFC) for reducing volume and parasitic power is designed and fabricated using several integrated technologies. New bipolar plates with tapered channels at the anode and a pillar array at the cathode are first applied to a passive micro-DMFC. The substrate of the bipolar plates made of acrylonitrile butadiene styrene (ABS) is hot embossed with two molds, fabricated by UV-LIGA and micro machining. To make the bipolar plates conductive and hydrophilic, a nickel layer is electroplated on the ABS plates, and three PDDA/PSS bi-layers are self-assembled onto the nickel layer. The bipolar plates are produced using hot embossing, a low cost, highly accurate batch process. A single cell is assembled to verify the self-pumping function, and it can generate a peak power density of 7.4 mW cm^{-2} with a 3 M methanol solution. The fuel cell is verified to work in three different orientations. When the fuel cell is placed horizontally, the self-pumping rate is about 0.1–0.15 mL h^{-1}. And the fuel cell can work through self-pumping for 5 h under this condition.

1. Introduction

Recently, with the demands of high energy density for commercial electronics and micro devices, micro direct methanol fuel cells (micro-DMFC) have been considered as a promising power source candidate instead of lithium-ion batteries. The investigation of micro-DMFC system is a hot topic both in academia [1–3] and industry [4–6]. Some companies even have launched their products or prototypes, such as Toshiba's Dynario in 2010 [6]. In theory, methanol has a dramatic energy density, 4878 Wh L^{-1} in volume and 6098 Wh kg^{-1} in weight. Based on the state-of-the-art, the fuel volume-based energy density of micro-DMFC prototypes could be 620–1420 Wh L^{-1}, much higher than the energy density of the Li-ion battery (about 350 Wh L^{-1}) [7]. However, the system volume-based energy density is quite low, normally 77–325 Wh L^{-1} [7]. One of the reasons for the low system volume-based energy density is that the ancillary components in the system consume part of the overall energy, and increase the entire volume and weight. The pump used to deliver liquid fuel in an active micro-DMFC is normally the main energy consuming source, especially when the scale of micro-DMFC is reduced to fit small portable devices. Sometimes, a pump may even use more energy than the fuel cell can generate. A passive micro-DMFC [8,9] may be an alternative choice, but the output power is limited by the low fuel delivering rate. Moreover, the fuel is mainly delivered by diffusion in a passive mode, so the anode electrode needs to be directly attached to the fuel reservoir, making the system incompatible and limited to a certain orientation.

In fact, the CO_2 bubbles generated from the electrochemical reactions contain some energy which can further push the capillary-driven liquid movement. Different approaches had been done to improve the mass transportation in micro-DMFC by using the energy [1,10–12]. Zhao and Ye [12] developed a passive fuel delivery system with the liquid fuel self-pumping by the CO_2 bubbles in a single serpentine flow field. By combining the theoretical and experimental results, they found that the methanol feeding system was capable of achieving a performance comparable to an active pump system for 0.5–4.0 M methanol. However, this micro-DMFC could have a selectivity of orientations, because the movement of bubbles is only along the effects of buoyancy. Their system requires a vertical pipe, and the effective height strongly affected the movements of bubbles. This problem was solved by applying some special microstructures in the flow fields. Meng and Kim [1] developed a silicon based self-pumping micro-DMFC. They built a gas-blocking element to make the bubbles moving towards one direction and venting through a porous silicon membrane. With the removal of CO_2 bubbles, a little fresh methanol solution will be vented into a flow field. Paust et al. [10,11] had a concept of degassing bubbles and self-pumping by the difference of capillary pressures. High feeding rate, 13 times higher than the methanol oxidation rate, was achieved

* Corresponding author.
** Corresponding author. Tel.: +1 612 626 1636.
E-mail address: tcui@me.umn.edu (T. Cui).

0378-7753/$ – see front matter © 2011 Elsevier B.V. All rights reserved.
doi:10.1016/j.jpowsour.2011.03.037

by applying parallel tapered channels with T-shape cross sections.

The self-pumping technique allows the designers to reconsider the design of a passive micro-DMFC from several aspects, including arrangement in a stack, series interconnection, materials, and fabrication. Since the reservoir need to be attached directly to the electrode in a passive micro-DMFC as mentioned above, each single cell was typically put into the same plane in traditional designs [8]. This made the stack incompact and complex in series interconnection. A bipolar plate structure can make the system compactable and easily interconnected without ultra wires. The bipolar plate structure means that the bipolar plate acts as an anode for one cell and a cathode for the next cell in a stack structure. This structure was applied to an active micro-DMFC stack [13,14]. However, it was considered very hard to be utilized in a passive stack [8,12], because the liquid fuel is difficult to be delivered into a flow field only by diffusion. The self-pumping technique can deliver the methanol solution into the flow field at a high rate without an ancillary pump. If the self-pumping technique can be integrated with the bipolar plate structure, the passive micro-DMFC would be more compactable and the series interconnection would be much easier.

With the integration of the self-pumping technique, bipolar plates may be much more different from the traditional one. Suitable material and fabrication methods will be required to meet the requirements for strength, accuracy, weight, and cost. Although microfabrication on silicon wafers is an attractive approach for its maturity and high accuracy, this method has been refuted many times because of its fragility, low conductivity, and high cost [8,15]. Stainless steel and titanium alloy may be suitable for the bipolar plates after a proper corrosion protection. Using wet chemical etching, micro structures can be efficiently fabricated at low cost [8,15], but the aspect ratio of the structures is limited. Compared with silicon and metal, polymer is an alternate material due to its manufacturing flexibility, chemical stability, and low cost. Using hot embossing, micro structures can be duplicated on polymer plates with high accuracy and low cost [16,17]. Although most of polymers are insulating, high conductivity can be achieved after a metallization on the polymers. Nguyen et al. [18] assembled a micro fuel cell with gold-sputtered polymethyl methacrylate (PMMA) substrates, on which the gas flow channels were formed by laser micromachining. Litterst et al. [10] used the hot embossing technique to fabricate transparent PMMA plate to observe the bubble development and movement. Due to the insulation of PMMA, stainless steel sheets machined by laser were used as a current collector in their experiments. However, sputtering is an expensive way to make polymer conductive, and the application of an extra current collector, stainless steel sheet, makes the assembly process more complex. Alternatively, a low cost metal layer can be easily deposited on a polymer substrate by an electrochemical deposition, especially on ABS (acrylonitrile butadiene styrene) [19].

In this paper, a new conception of a self-pumping micro-DMFC stack, assembled with metalized polymer bipolar plates, is presented. A simple model was used to explain the mechanism of self-pumping. New bipolar plates were fabricated using several techniques, including UV-LIGA, metallization of polymer, and nano self-assembly. With the bipolar plates, micro-DMFCs were assembled, and tested under different methanol concentrations along different orientations. In addition, the self-pumping rate was characterized.

2. Self-pumping mechanism and design of fuel cell stack

2.1. Self-pumping mechanism

When a CO_2 bubble is generated from the electrochemical reaction, it enters into a channel through a gas diffusion layer, and moves towards an open area of the channel to minimize surface energy. Fresh fuel can be sucked into the channel from the narrow end, when the bubble is traveling along the channel like a piston. This mechanism is similar to the oxygen bubble movement presented by Maharbiz et al. [20].

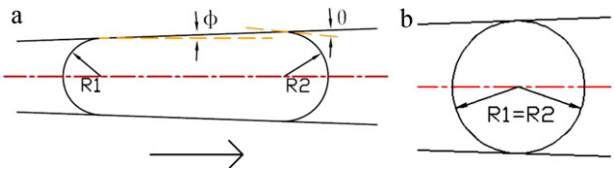

Fig. 1. Tapered micro-channel bubble geometry: (a) nonequilibrium state and (b) equilibrium state.

When a bubble is introduced into a tapered channel with hydrophilic surface, as shown in Fig. 1, two opposite but unbalanced forces are applied to each end of the bubble. The difference is due to the change of channel cross section. The following equations describe the force on each ends of the bubble

$$F_1 = 2R_1\pi\sigma \cos(\theta + \phi) \quad (1)$$

$$F_2 = 2R_2\pi\sigma \cos(\theta - \phi) \quad (2)$$

where F_1 and F_2 are the forces on each end of the bubble, R_1 and R_2 are the radius of gas/liquid interface, σ is the surface tension, θ is the contact angle, and Φ is the angle between the channel wall and the channel axis. By combining Eqs. (1) and (2), the total force along the central line is:

$$F = 2\pi\sigma[R_2 \cos(\theta - \phi) - R_1 \cos(\theta + \phi)] \quad (3)$$

For a completely hydrophilic material ($\theta = 0^\circ$), the net driving force is given by

$$F = 2\pi\sigma \cos(\phi)[R_2 - R_1] \quad (4)$$

From Fig. 1a, it is obvious that F will be more than 0 until R_2 is equal to R_1. The bubble will continue to move until the two radiuses, R_1 and R_2, are the same, as shown in Fig. 1b.

Moreover, the continuous generation of CO_2 bubbles will also push the liquid moving due to the expansion of volume. Although the bubble may be blocked in the channel when it is in an equilibrium state ($R_1 = R_2$), other bubbles will be generated from the continuous electrochemical reaction. The volume of the bubble will be expanded due to the coalescence, thus the bubble will continue to move until the next equilibrium state. If the bubble reaches an open end, it will be no longer limited by the channel and float out.

2.2. Structure of bipolar plates

The bipolar plates used in a micro-DMFC were metalized polymer plates with anode and cathode flow fields on each side, as shown in Fig. 2a. ABS was formed by hot embossing, followed by electroplating of nickel. The anode flow field consisted of 15 parallel tapered channels with 250 μm depth. Each channel was a straight channel (110 μm wide and 4.3 mm long) with a tapered channel (110 μm wide at narrow end, 580 μm wide at wide end, and 26.7 mm long), as shown in Fig. 2b. For the cathode, there is a pillar array (1 mm in diameter and 1 mm high with a pitch of 1.5 mm) in the middle of a plate. Four screw holes, 2.7 mm in diameter, were used to assemble and seal the fuel cell, and another four vias (0.5 mm in diameter) were used to connect the nickel layer on each side of the plate.

2.3. Stack design

Fig. 3 shows the structure of the micro-DMFC assembled with bipolar plates. Membrane electrode assemblies (MEAs) with

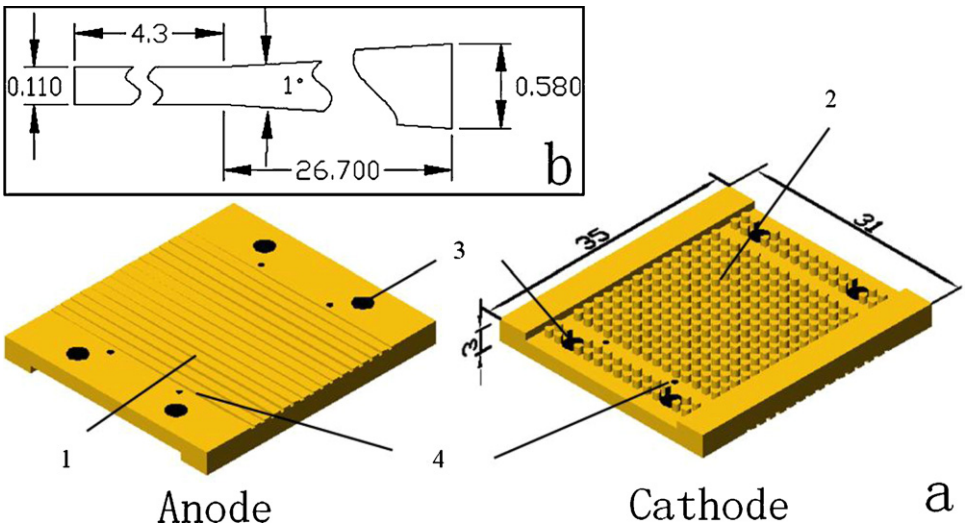

Fig. 2. Schematic of bipolar plates: (a) 3D view of a bipolar plate (1, anode flow field; 2, cathode flow field; 3, screw holes; 4, vias) and (b) scales of the tapered channel.

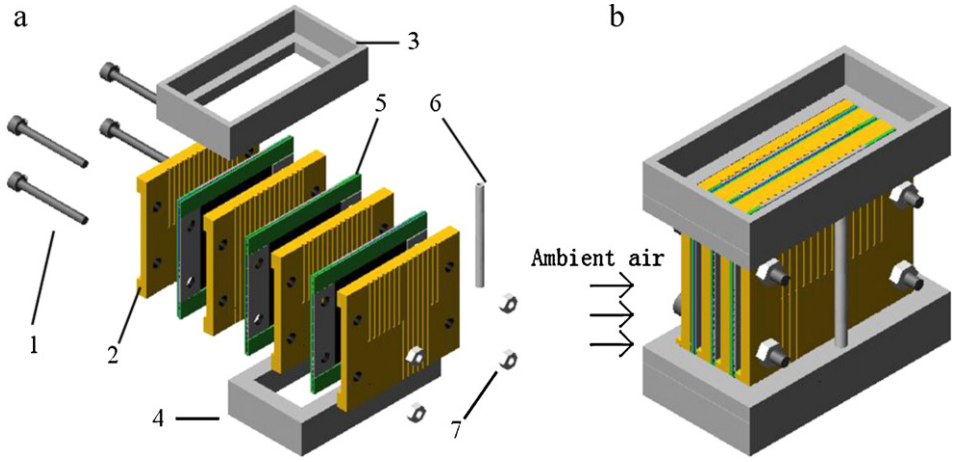

Fig. 3. Schematic of the micro-DMFC stack: (a) exploded view of the self-pumping DMFC (1, bolts; 2, bipolar plates; 3, reservoir 1; 4, reservoir 2; 5, MEA with sealant; 6, pipe; 7, nuts) and (b) extended micro-DMFC stack.

sealant and bipolar plates were sandwiched one by one together with bipolar plates as the end plates. All the plates were aligned with the channels at the same direction. Four M2 bolts were assembled through the bipolar plates and MEAs and were fasten with nuts. Two reservoirs were connected with the channels, reservoir 1 as the wide outlet and reservoir 2 as the narrow inlet. The two reservoirs were also connected with a plastic pipe with a 2 mm inside diameter. When the micro-DMFC was working, CO_2 bubbles were generated on catalyst, and transferred into the channels through the gas diffusion layer. The bubbles moved from the narrow inlet to the wide outlet, and flowed into reservoir 1, making a little methanol solution sucked from reservoir 2. Meanwhile, the methanol solution will be replenished by reservoir 1 through the plastic pipe. On the cathode side, the ambient air was transferred to the electrodes through the gap constructed by the pillar arrays.

3. Experimental

3.1. Mold fabrication

A cathode mold and an anode mold were fabricated for the hot embossing. The anode mold was electroformed by the UV-LIGA, as shown in Fig. 4. Firstly, 50 nm Cr and 100 nm Au were sputtered on a piece of 4-in. silicon wafer. Next, about 250 μm SU8 3050 (Microchem, USA) was spin coated on a wafer at a speed of 700 rpm for 40 s, followed by a soft-baking at 65 °C for 7 min and 95 °C for 60 min. A film mask was used to transfer patterns to photoresist using a contact photolithograph for 60 s with a light power density of 1.2 mW cm^{-2}. After exposure, the wafer was post-baked on a hot plate at 95 °C for 20 min, and developed in propylene glycol monomethyl ether acetate (PGMEA) for about 30 min. In step 4, the wafer was electroformed in a sulfamate nickel solution as illustrated in Table 1 until the channels were filled. With a shadow mask machined by laser, 30 nm Au layer was sputtered to make SU8 conductive. The wafer was electroformed until nickel was thicker than 3 mm. The silicon was removed using a KOH solution, and the SU8 was removed using SU8 Remover (Microchem, USA) at

Table 1
Parameters of nickel electroplating.

Parameters	Value
Ni^{2+}	90 g L^{-1}
Boric acid	40 g L^{-1}
pH	4
Temperature	57 °C
Current density	2 A dm^{-2}

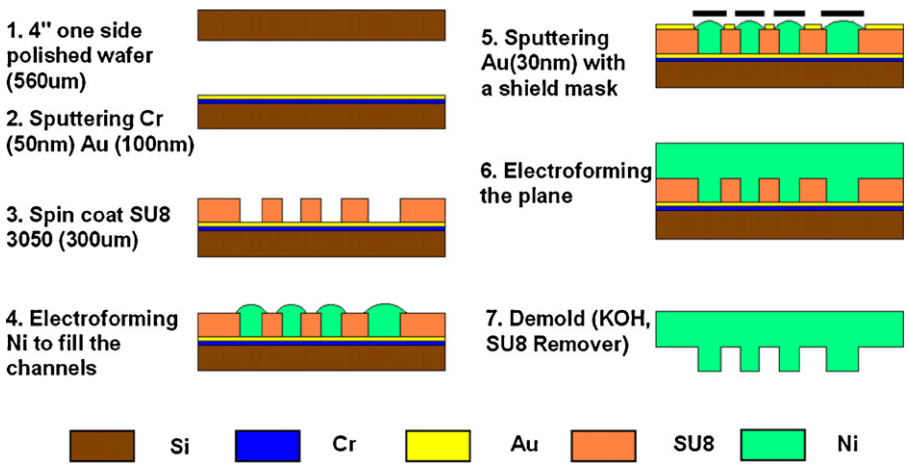

Fig. 4. Process flow chart of the anode mold.

90 °C. Finally, the mold was machined into a rectangular shape, as shown in Fig. 5a. Fig. 5b shows the cathode mold machined by a micro miller. The cathode mold 51 mm × 61 mm × 6 mm was made of stainless steel.

3.2. Fabrication of bipolar plates using hot embossing

Bipolar plates with microstructures on both sides were fabricated through double side hot embossing [21] process using HEX01 (JEONOPTIK Microtechnik GmbH, Germany) with the anode and cathode molds, shown as in Fig. 5. The hot embossing process was described as follows. Firstly, an ABS plate was sandwiched between the aligned anode and cathode molds installed on bottom and top hot plates in HEX01. A rotary pump connected to the embossing chamber provided a vacuum lower than 0.1 mbar to prevent air bubbles in the embossed polymer. The ABS and the molds were heated up to 140 °C, which was 60 °C above the glass transition temperature. A molding force of 15 kN was applied to an area of 50 mm × 50 mm for a duration of 300 s until the filling process was finished. The molding force remained on the molds while they were cooling down. When the temperature decreased to 85 °C, the molding force was released, and the sample was taken out. The ABS bipolar plate, as shown in Fig. 6, was manually detached from the molds and machined into a regular shape. The four vias were also drilled in the last step.

3.3. Metallization of the bipolar plates

The ABS bipolar plates were metalized by several chemical and electrochemical steps. Firstly, the plates were baked in an oven under 65 °C for 2 h to release stress. High stress may cause the metal layer peeling off from the plastic. Secondly, the plates were immersed in methanol for 1 min to remove oil, and rinsed with DI water. Sequentially, a mixture of CrO_3 (400 g L^{-1}) and H_2SO_4 (330 mL L^{-1}) was used as an etchant to roughen the surface at 65 °C for 20 min. The solution can dissolve the rubber elastomer phases of the ABS graft polymer, resulting in a rough surface with micro pores [17]. The micro cavities were served to achieve anchors for a good adhesion of coatings. A little hexavalent chromium may exist in the cavities and affect the coating of Sn^{2+} in the next step, thus the plates were deoxidized in Na_2SO_3 (20 g L^{-1}) for 1 min and rinsed with DI water. Because the screws may make the fuel cell short circuit, part of the plate should be prohibited from the solution. An agar solution (6 g L^{-1}, 80 °C) as a gel at room temperature were brushed on the plates using a brush pen. The plates were immersed in a mixture of $SnCl_2$ (20 g L^{-1}) and HCl acid (40 mL L^{-1}) to make Sn^{2+} adhered to the surface. After being rinsed with DI water, the plates were put into a silver–ammonia solution with 3 g L^{-1} $AgNO_3$. Sn^{2+} can reduce Ag^+ to metal Ag, which would be a catalyst for the chemical plating of copper. Next, the plates were put into a formaldehyde solution (100 mL L^{-1}) to reduce ultra Ag^+ ion.

A layer of copper was chemically deposited on the plates as a seed layer before electroplating. The solution was mixed with $CuSO_4{\cdot}5H_2O$ (20 g L^{-1}), $C_4H_4KNaO_6{\cdot}4H_2O$ (potassium

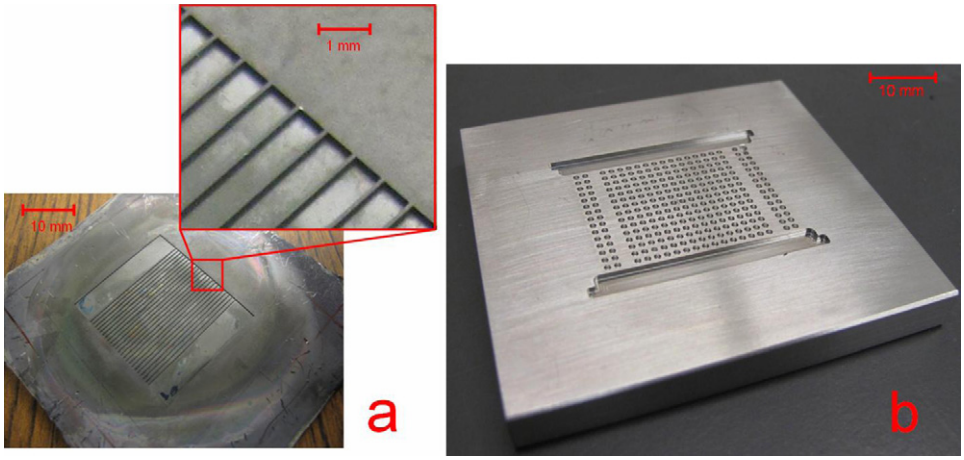

Fig. 5. Photos of anode and cathode molds: (a) anode mold and (b) cathode mold.

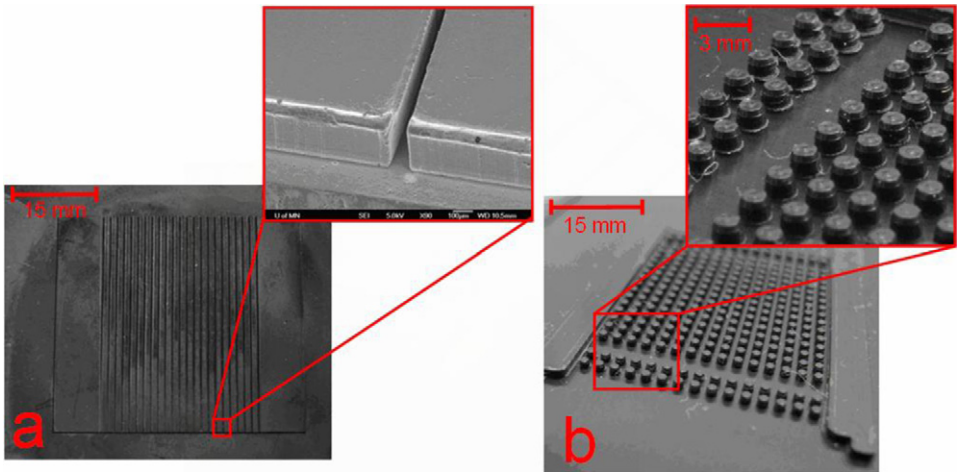

Fig. 6. Photos of bipolar plates after hot embossing: (a) anode flow filed and (b) cathode flow filed.

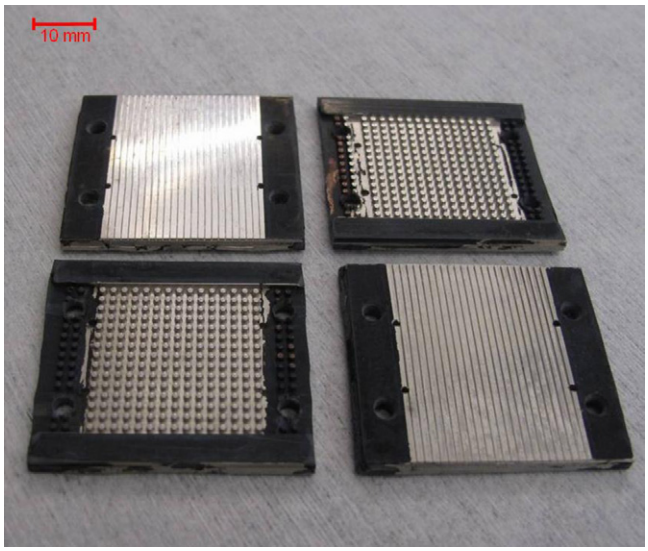

Fig. 7. Partly electroplated ABS bipolar plates.

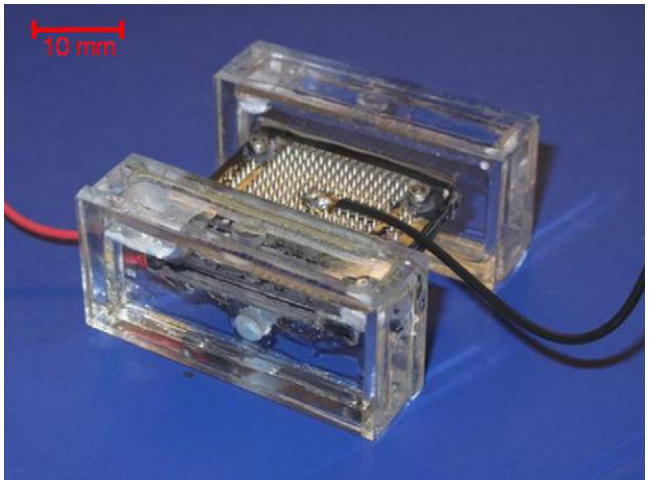

Fig. 9. Photo of an assembled micro-DMFC.

sodium tartrate tetrahydrate, 60 g L^{-1}), NaOH (30 g L^{-1}), Na_2CO_3 (15 g L^{-1}), and formaldehyde (10 mL L^{-1}). The first three chemicals should be mixed in advance. After adding formaldehyde into the mixture, copper is deposited on the plates. The plates were chemically plated in the solution for 20 min. Finally, the plates were rinsed with water at 80 °C to remove residuals.

The plates were electroplated in the same nickel electroplating solution in Table 1. To get double sides electroplated, two nickel plates were put face to face in a beaker and connected together as an anode, and the plate was electroplated in the middle. The current density was 3 A dm^{-2}. After electroplating for 6 min, the thickness of nickel layer was about 5 μm. The last step was to block the vias by epoxy. Fig. 7 shows the partly metallized bipolar plates, on which the black part is insulated ABS, and the silver part is the conductive nickel layer.

3.4. Surface modification

The surface of the channels should be modified to super hydrophilic to fit the mold in 2.1, in which θ should be 0°. Due to the weak hydrophilic nature of the nickel layer, the channels were hard to be infiltrated by the methanol solution, as shown in Fig. 9b.

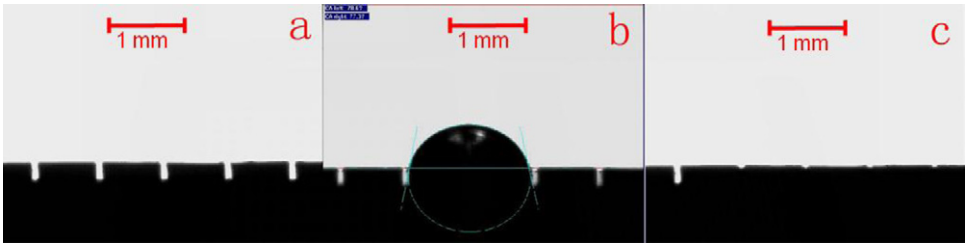

Fig. 8. Hydrophilicity of the bipolar plates: (a) cross section of a bipolar plate (from the narrow end); (b) contact angle on a plate without PDDA/PSS and (c) a fully infiltrated plate with PDDA/PSS.

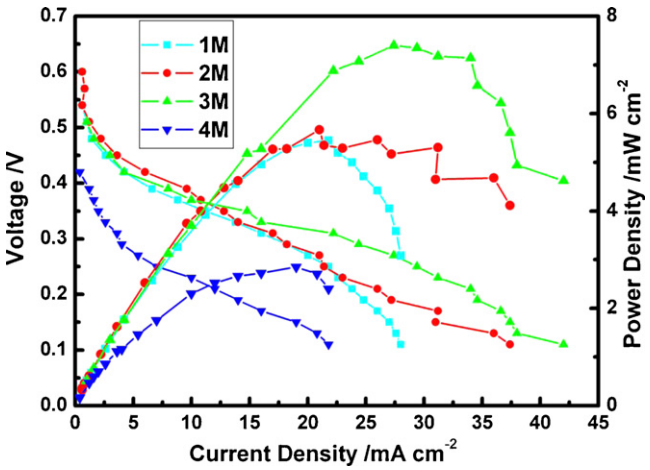

Fig. 10. *I–V* curves and *I–P* curves under different methanol concentrations.

To make the channel hydrophilic, three bi-layers of polymers were self-assembled on the plates. The bipolar plates were immersed in 1.5 wt.% poly diallyldimethylammonium chloride (PDDA) dispersion with 0.5 M NaCl for 15 min at room temperature, followed by rinsing with DI water. The bipolar plates then were dipped into 0.3 wt.% poly styrene sulfonate (PSS) with 0.5 M NaCl for 15 min and rinsed. The PDDA/PSS adsorption treatment was repeated for three cycles, and finally treated with PSS. The contact angle was changed from 78° to 0° after the PDDA/PSS coating, as shown in Fig. 8.

3.5. Assembly of micro-DMFC

To verify the design in 2.3, a stack with a single cell was assembled, as shown in Fig. 9. A piece of commercial MEA (Fuel Cell Store, USA) with an active area of 5 cm^2 (2.24 cm × 2.24 cm) was sandwiched between two bipolar plates. The MEA had 2 mg Pt cm^{-2} loaded at the cathode and 4 mg Pt–Ru cm^{-2} loaded at the anode. Nafion 117 was used as the proton exchange membrane. PTFE sealant (Gore-Tex, Germany) was used to seal the fuel cell. With epoxy, two reservoirs (51 mm × 25 mm × 12 mm) formed by polymethyl methacrylate (PMMA) were fixed on each side. The two power cords were soldered on the outside of the bipolar plates to simulate the connection of a stack with multiple pieces of MEA.

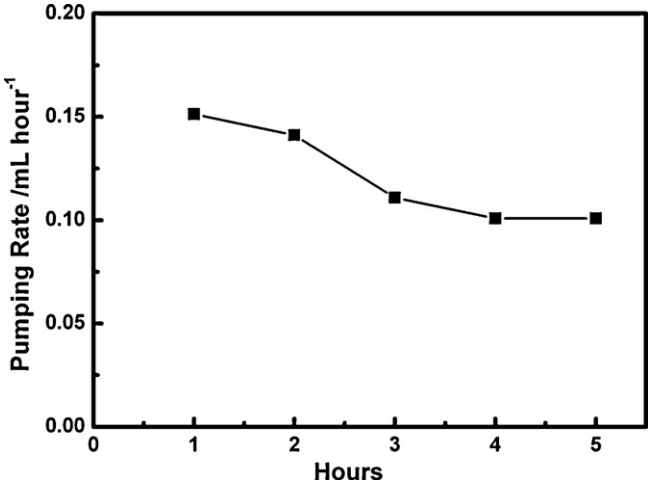

Fig. 11. Self-pumping rate for 5 h.

Table 2
Data of fuel volume consumed during 5 h.

	Pumping rate based data (mL)	Current based data (mL)
Fuel volume pumped in the flow field	0.605	
Fuel volume already in the flow field	0.035	
Total	0.64	0.775

4. Results and discussions

4.1. Influence of methanol concentration

The micro-DMFC was tested with a DC electronic load (IT8500, BK Precision, USA) at room temperature and ambient pressure. The micro-DMFC was laid horizontally to eliminate the effects of buoyancy, as shown in Fig. 9. The reservoirs were filled with methanol solution, flowing into the channels by capillary. The performance comparison of the fuel cell with different methanol concentrations is shown in Fig. 10. The peak power density increases from 5.5 mW cm^{-2} to 7.4 mW cm^{-2} when the concentration of methanol changes from 1 M to 3 M. This is because more methanol molecules can be catalyzed on the surface of catalyst when using higher concentrated methanol. However, the peak power density drops to 2.9 mW cm^{-2}, when the fuel concentration is 4 M. The reason is that the effect of the potential generated from methanol crossover exceeds that of the concentration of methanol molecules close to catalyst. Moreover, the 1 M fuel has a similar peak power density as the 2 M fuel, however, the 1 M fuel has a typical concentration polarization when the current density is more than 20 mA cm^{-2}. This is because the methanol molecules have to diffuse through a gas diffusion layer, making the concentration nearby the catalyst lower than the concentration in the channels. When the current density is more than 20 mA cm^{-2}, the diffusion speed for the 1 M fuel is lower than the electrochemical reaction speed, therefore the current is limited. For the 2 M fuel, there was not an obvious concentration polarization. This is because the mass of methanol feed in the channels is twice than the 1 M fuel during the self-pumping. The concentration of methanol is enough for the electrochemical reaction when a 2 M methanol solution is applied.

4.2. Self-pumping rate

The self-pumping rate was measured for 5 h using the following approach. Two pieces of PTFE tape were used to seal the plastic pipe, and the two reservoirs were filled with 2 M methanol to the same level, so that the solution would not flow between them. The fuel cell was arranged horizontally to run at a current of 50 mA for 1 h, while the solution level at reservoir 2 was reduced. A needle tube with a 2 M methanol solution was weighed by a balance, and the solution was used to refill the reservoir. The methanol solution weight filled in the reservoir was determined by subtracting the needle tube weight. The pumping rate was reduced from 0.15 mL h^{-1} to 0.1 mL h^{-1} for a testing duration of 5 h.

The current based data was compared with the pumping rate based data to verify the function of self-pumping. Table 2 shows the different data of the fuel volume consumed during 5 h. The fuel volume pumped into the flow field is a summary from Fig. 11. The fuel volume already in the flow field is calculated from the total volume of 15 tapered channels. The current based data was calculated

Table 3
The bubble moving under different orientations.

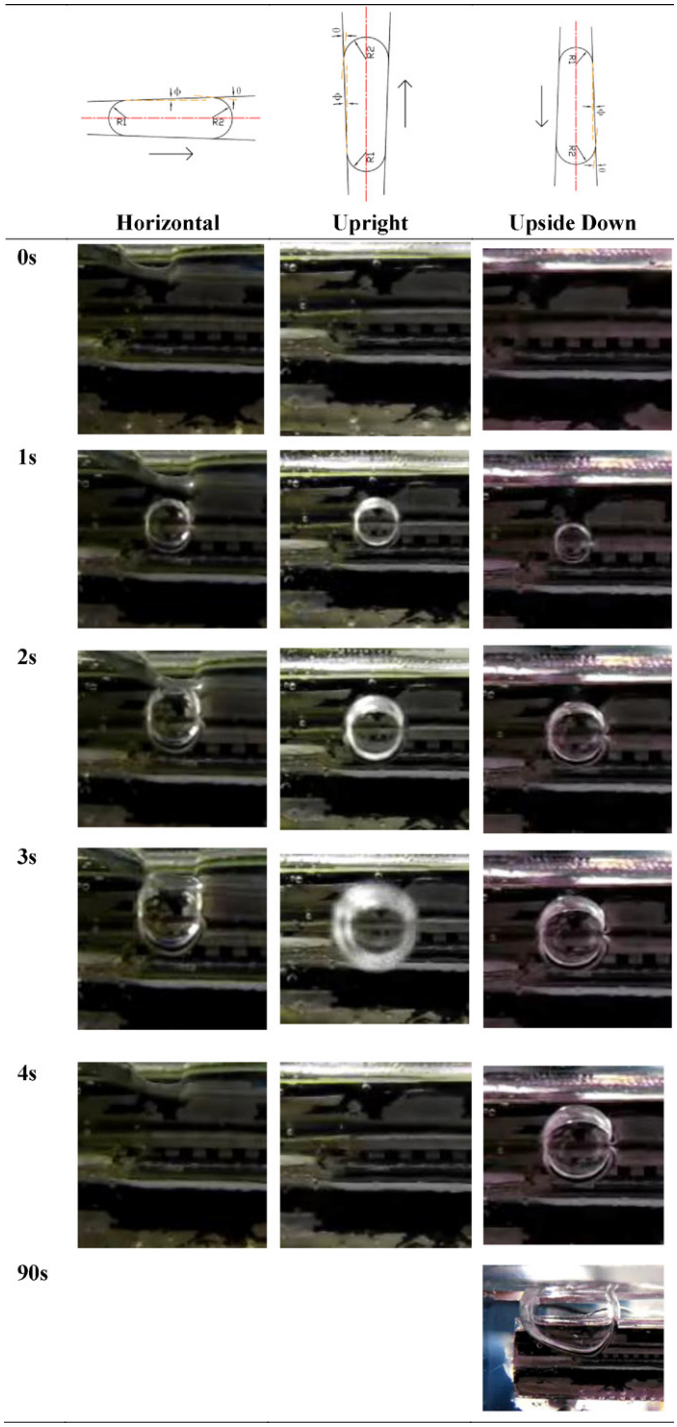

by

$$V_M = \frac{It}{6C_M F} \quad (5)$$

where V_M is the volume of fuel, I is the current, t is the time, C_M is the concentration of methanol, and F is the Faraday constant. It is easy to determine that the fuel consumed during 5 h is more than what already existed in the flow field. Therefore, the fuel cell must depend on the supply from the reservoir to work continuously for 5 h. Moreover, the fuel volume pumped into the flow field is a little lower than the current based data. This is because the fuel is not only siphoned from the narrow end. The fuel can partially diffuse or be sucked from the wide end connected with reservoir 1.

4.3. Effects of orientation

The micro-DMFC was tested along three different orientations, horizontal, upright and upside down. Horizontal position means that the channels were placed horizontally to exclude the effect of buoyancy. Upright position means that the channels were oriented vertically with wide end on top, thus the bubbles can be pushed out with the aid of buoyancy. Upside down position is an opposite orientation of upright, where the bubble should overcome the buoyancy during movement. The fuel cell was under an electronic load at a current of 50 mA with a 2 M fuel supply. A digital camera (G10, Cannon, Japan) was used to record the video of a bubble movement. As shown in Table 3, the bubble in the channels can be pushed out under all orientations. Especially when oriented upside down, the bubble can overcome the buoyancy during its movement. Moreover, the time for the bubble separated from the channel end is different. The bubble generated in upright orientation was separated from the channel after 3 s, as shown in Table 3. It was a little faster than that in horizontal orientation, because the buoyancy can shorten the duration of bubble movement and separation. For the upside down orientation, the bubble volume was continuously increased, but it is very hard to be separated. This is because the bubble was stopped by the top plate of the reservoir, as shown in the image at the 90th second in Table 3.

5. Conclusions

We demonstrated and verified a self-pumping micro-DMFC with polymer bipolar plates, making a methanol solution circulated using the energy from the expansion of carbon dioxide. The mechanism of self-pumping was explained by a simple two phase fluid model. Several micro- and nano-fabrication techniques combined with chemical and electrochemical methods were used to fabricate the bipolar plate. Using the bipolar plates, a single cell with an active area of 5 cm^2 was assembled and tested. A peak power density of 7.4 mW cm^{-2} was achieved with a 3 M methanol solution at air ambient. The self-pumping rate can reach 0.1–0.15 mL h^{-1} at a current of 50 mA when the fuel cell was placed horizontally. The fuel cell worked along different orientations, even making the bubble moving when the channel was placed upside down. The new self-pumping fuel cell can reduce the volume, simplify the electrical connections, and omit an extra pump to circulate the fuel.

Acknowledgments

This research is partially sponsored by the Technology Integration of Advanced Nano/Microsystem Laboratory at the University of Minnesota and the National Natural Science Foundation of China (Nos. 50805013 and 50905027).

References

[1] D.D. Meng, C.J. Kim, J. Power Sources 194 (2009) 445–450.
[2] S. Tominaka, S. Ohta, H. Obata, T. Momma, T. Osaka, J. Am. Chem. Soc. 130 (2008) 10456–10457.
[3] H. Joh, T.J. Ha, S.Y. Hwang, J.H. Kim, S.H. Chae, J.H. Cho, J. Prabhuram, S.K. Kim, T.H. Lim, B.K. Cho, J.H. Oh, S.H. Moon, H.Y. Ha, J. Power Sources 195 (2010) 293–298.
[4] http://www.mtimicrofuelcells.com.
[5] http://techon.nikkeibp.co.jp/english/NEWS_EN/20080502/151303/.
[6] http://www.toshiba.co.jp/about/press/2009_10/pr2201.htm.
[7] T.S. Zhao, W.W. Yang, R. Chen, Q.X. Wu, J. Power Sources 195 (2010) 3451–3462.
[8] Y. Zhu, J. Liang, C. Liu, T. Ma, L. Wang, J. Power Sources 193 (2009) 649–655.

[9] W.M. Yang, S.K. Chou, C. Shu, J. Power Sources 164 (2007) 549–554.
[10] C. Litterst, S. Eccarius, C. Hebling, R. Zengerle, P. Koltay, J. Micromech. Microeng. 16 (2006) 248–253.
[11] N. Paust, C. Litterst, T. Metz, M. Eck, C. Ziegler, R. Zengerle, P. Koltay, Microfluid Nanofluid 7 (2009) 531–543.
[12] Q. Ye, T.S. Zhao, J. Power Sources 147 (2005) 196–202.
[13] A Oedegaard, C. Hentschel, J. Power Sources 158 (2006) 177–187.
[14] H.I. Joh, S.Y. Hwang, J.H. Cho, T.J. Ha, S.K. Kim, S.H. Moon, H.Y. Ha, Int. J. Hydrogen Energy 33 (2008) 7153–7162.
[15] G.Q. Lu, C.Y. Wang, J. Power Sources 144 (2005) 141–145.
[16] M. Heckele, W. Bacher, K.D. Muller, Microsyst. Technol. 4 (1998) 122–124.
[17] H. Becker, U. Heim, Sens. Actuators A 83 (2000) 130–135.
[18] S.H. Chan, N. Nguyen, Z. Xia, Z. Wu, J. Micromech. Microeng. 15 (2005) 231–236.
[19] R. Suchentrunk, Metallizing of Plastics: A Handbook of Theory and Practice, Materials Park, Ohio, 1993.
[20] M.M. Maharbiz, W.J. Holtz, S. Sharifzadeh, J.D. Keasling, R.T. Howe, J. Microelectromech. S12 (2003) 590–599.
[21] J.H. Chang, S.Y. Yang, Microsyst. Technol. 10 (2003) 76–80.